Journal of Computational Physics 374 (2018) 654–667

Contents lists available at ScienceDirect

Journal of Computational Physics

www.elsevier.com/locate/jcp

Efficient local energy dissipation preserving algorithms for the Cahn–Hilliard equation

Zhenguo Mu [a], Yuezheng Gong [b], Wenjun Cai [a], Yushun Wang [a,*]

[a] Jiangsu Key Laboratory of NSLSCS, School of Mathematical Sciences, Nanjing Normal University, Nanjing 210023, PR China
[b] College of Science, Nanjing University of Aeronautics and Astronautics, Nanjing 210016, PR China

ARTICLE INFO

Article history:
Received 8 March 2018
Received in revised form 1 August 2018
Accepted 1 August 2018
Available online 4 August 2018

Keywords:
Cahn–Hilliard equation
Mass conservation
Local energy dissipation law
Local structure-preserving algorithm
Total energy dissipation law

ABSTRACT

In this paper, we show that the Cahn–Hilliard equation possesses a local energy dissipation law, which is independent of boundary conditions and produces much more information of the original problem. To inherit the intrinsic property, we derive three novel local structure-preserving algorithms for the 2D Cahn–Hilliard equation by the concatenating method. In particular, when the nonlinear bulk potential $f(\phi)$ in the equation is chosen as the Ginzburg–Landau double-well potential, the method discussed by Zhang and Qiao (2012) [50] is a special case of our scheme II. Thanks to the Leibnitz rules and properties of operators, the three schemes are rigorously proven to conserve the discrete local energy dissipation law in any local time–space region. Under periodic boundary conditions, the schemes are proven to possess the discrete mass conservation and total energy dissipation laws. Numerical experiments are conducted to show the performance of the proposed schemes.

1. Introduction

There has been an increasing emphasis on the free interface problem of multi-phase incompressible flows which is often modeled by the diffuse interface method with a long history [39,44]. Its main idea is to apply one or more continuous functions to describe the volume fraction in the multi-phase immiscible system and represent the fluid interfaces by a thin and smooth transition layers, see, e.g., [1,3,7,20,22,33,34,37,47] and [38,43] for details. The Cahn–Hilliard equation induced by the variational approach, is a widely used phase-field model.

In this paper, we consider the following Cahn–Hilliard (CH) equation [6]

$$\begin{cases} \frac{\partial \phi}{\partial t} = \Delta \mu, \\ \mu = f'(\phi) - \kappa \Delta \phi, \end{cases} \tag{1.1}$$

where ϕ is an unknown real-valued phase function, which stands for the relative concentration of one phase, μ is the chemical potential which is the variation of the free energy, κ is a parameter measuring the strength of the conformational entropy. Here the free energy is chosen as

* Corresponding author.
E-mail address: wangyushun@njnu.edu.cn (Y. Wang).

https://doi.org/10.1016/j.jcp.2018.08.004
0021-9991/

$$E[\phi] = \int_{\Omega} \left(\frac{\kappa}{2} |\nabla \phi|^2 + f(\phi) \right) d\mathbf{x}, \tag{1.2}$$

where Ω is the domain that the fluid occupies, and $f(\phi)$ is the bulk energy density. For the choice of nonlinear potential $f(\phi)$, Ginzburg–Landau double-well type potential,

$$f(\phi) = \frac{\gamma}{4}(1-\phi^2)^2, \ \ \phi \in [-1, 1],$$

and Logarithmic Flory–Huggins potential [41],

$$f(\phi) = \gamma(\phi - \phi^2) + (1-\phi)\ln(1-\phi) + \phi \ln \phi, \ \ \phi \in [0, 1],$$

are two widely used nonlinear bulk potentials in the literature, where γ measures the strength of the repulsive potential. As is well known, the CH equation, with suitable boundary conditions, possesses the mass conservation law (MCL)

$$I(t) := \int_{\Omega} \phi(\mathbf{x}, t) d\mathbf{x} \equiv I(0), \tag{1.3}$$

and the energy dissipation law (EDL)

$$\frac{dE}{dt} = -\int_{\Omega} |\nabla \mu|^2 d\mathbf{x}. \tag{1.4}$$

To date, extensive mathematical studies have been carried out for the CH equation, see, e.g., [7–10,19,21,31,32,37,40,42,47] for details. For the analytical front, the steady state solution, the existence and the uniqueness of the system, we refer to [13,24] and the references therein. For the numerical front, various numerical methods have been considered in the literature. Elliott et al. [12] discussed the physical background and its numerical solution by the Galerkin finite element method. Later, Feng and Prohl [17] developed the mixed finite element method which was convergent with quasi-optimal order in time and optimal order in space. Sun [40] proposed the finite difference method by the method of reduction of order, which is conditionally stable and not mass conserving. Choo et al. [5] gave a conservative nonlinear finite difference scheme, which was proven to preserve the total mass, yet the energy-based stability was not discussed. Subsequently, Furihata [16] gave a conservative finite difference scheme, which was proven to be unconditionally stable in the sense of energy decay. Chen and Shen [8] developed a semi-implicit Fourier spectral scheme, in which the linear part was treated implicitly and the nonlinear part was calculated explicitly. Later, Zhu et al. [49] proposed the semi-implicit Fourier spectral method for the CH equation with a variable mobility. Shen and Yang [42] obtained energy stability method without any a priori assumption on the numerical solution. Zhang and Qiao [50] discussed a finite difference scheme and proposed an adaptive time-stepping technique to quickly solve the 2D CH equation. He et al. [31] proposed a large time-stepping methods. Guo et al. [27] used the convex splitting skills, whose idea was proposed more than two decades earlier by Elliott et al. and Eyre in Ref. [14,15]. Li et al. [35,36] developed the semi-implicit Fourier spectral method, which was proved unconditional energy stability for modified energy functionals by the new stabilization techniques. Recently, the new technique called "Invariant Energy Quadratization" (IEQ) which was successfully applied to different phase-field models by authors [30,46,48], was extended to handle the CH equation in Ref. [25,26]. The efficient iterative solution of linear system was investigated for the coupled Navier–Stokes Cahn–Hilliard system, in which the block-triangular preconditioners were introduced in Ref. [2]. Gomez et al. gave a good reference book for stable time integration of phase-field equations in Ref. [23]. We notice that most existing methods and their stabilities which are discussed in the literature are based on the global energy dissipation property which is defined on the global space region and depends on the suitable boundary conditions. Here in this paper, we explore to construct novel schemes basing on our observation that CH equation has a local energy dissipation law which is valid in any time–space region and independent of the boundary conditions. It is known that boundary condition of the system is very important in many practical problems.

Proposition 1. *The system* (1.1) *possesses the local energy dissipation law (LEDL)*

$$\partial_t \left(\frac{\kappa}{2} |\nabla \phi|^2 + f(\phi) \right) - \nabla \cdot \left(\kappa \phi_t \nabla \phi + \mu \nabla \mu \right) + |\nabla \mu|^2 = 0, \tag{1.5}$$

which can be derived by multiplying μ and ϕ_t to the first line and the second line of (1.1) *respectively, and adding the two resluting formulas together. Compared with* (1.4)*, the LEDL* (1.5) *has an additional flux term which can supply much more information of the original system. Moreover, the LEDL is independent of boundary conditions. Therefore, it is valid in any time space domain for the CH equation with any boundary condition. Under suitable boundary conditions, the LEDL* (1.5) *implies the total EDL* (1.4)*. This observation motivates us to construct numerical schemes preserving the LEDL* (1.5) *for the CH equation.*

Actually, how to construct numerical schemes preserving certain local invariant quantities for the continuous dynamical systems is brought into sharp focus in recent years. The numerical methods preserving some structural properties of the

system are sometime referred as geometric integrators or structure-preserving numerical methods. So far, on construction of the local structure-preserving schemes for some classical PDEs, many results have been achieved [28,45] which further show that numerical methods with local property supply richer information of the original system than that of schemes with global property.

In this paper, we aim to construct three novel numerical schemes to preserve discrete analogues of the local energy dissipation law (1.5) for the 2D Cahn–Hilliard equation which are achieved through the concatenation of basic algorithms suggested by Wang et al. [45], including the implicit midpoint method, the leap-frog method and the discrete variational derivative method proposed by Furihata et al. [11,18] for the nonlinear term, on the associated first-order subsystems. The corresponding discrete local energy dissipation laws are rigorously proved by the Leibnitz rules, with no dependence of the boundary conditions. While imposed of the periodic boundary condition or the homogeneous boundary condition, the proposed schemes thereby possess the global EDL as well as MCL.

The remainder of this paper is arranged as follows. Some operator definitions and theirs properties are given in Section 2. In Section 3, we construct three novel numerical schemes preserving the LEDL for solving the CH equation. When the equation is imposed on appropriate boundary conditions, the schemes will conserve the global MCL and EDL. Numerical experiments are presented in Section 4 and some concluding remarks are given in the final section.

2. Operator definitions and properties

To simplify the presentation, we introduce some notations firstly. For a positive integer N_t, we define the time-step as $\Delta t = T/N_t, t_n = n\Delta t, 0 \le n \le N_t$. Let N_x, N_y be two positive integers. The spatial domain $\Omega = [x_L, x_R] \times [y_L, y_R]$ is uniformly partitioned with mesh size $h_x = (x_R - x_L)/N_x, h_y = (y_R - y_L)/N_y$ and

$$\Omega_h = \left\{(x_j, y_k) | x_j = x_L + jh_x,\ y_k = y_L + kh_y, 0 \le j \le N_x, 0 \le k \le N_y\right\}.$$

The approximation of the value of the function $f(x, y, t)$ at the node (x_j, y_k, t_n) is denoted by $f^n_{j,k}$. A grid function $f = \left\{f_{j,k} | j, k \in \mathbb{Z}\right\}$ is called periodic if

$$(x\text{-periodic})\ f_{N_x+j,k} = f_{j,k};\ (y\text{-periodic})\ f_{j,N_y+k} = f_{j,k}.$$

In order to derive the algorithms conveniently, we also give some definition of operators. Define the finite difference operators

$$\delta_t f^n_{j,k} = \frac{f^{n+1}_{j,k} - f^n_{j,k}}{\Delta t}, \quad \delta_x f^n_{j,k} = \frac{f^n_{j+1,k} - f^n_{j,k}}{h_x}, \quad \delta_y f^n_{j,k} = \frac{f^n_{j,k+1} - f^n_{j,k}}{h_y},$$

and averaging operators

$$A_t f^n_{j,k} = \frac{f^{n+1}_{j,k} + f^n_{j,k}}{2}, \quad A_x f^n_{j,k} = \frac{f^n_{j+1,k} + f^n_{j,k}}{2}, \quad A_y f^n_{j,k} = \frac{f^n_{j,k+1} + f^n_{j,k}}{2}.$$

We also define discrete inner product and norm for tensor valued functions as follows

$$(\mathbf{F}, \mathbf{G})_h = \sum_{m,n} \sum_{j=0}^{N_x-1} \sum_{k=0}^{N_y-1} (\mathbf{F}_{m,n})_{j,k} (\mathbf{G}_{m,n})_{j,k} h_x h_y, \quad \|\mathbf{F}\|_h = (\mathbf{F}, \mathbf{F})_h^{\frac{1}{2}}.$$

The operators have the following properties:

- Commutative law:

$$\delta_\alpha \delta_\beta f^n_{j,k} = \delta_\beta \delta_\alpha f^n_{j,k}, \quad A_\alpha A_\beta f^n_{j,k} = A_\beta A_\alpha f^n_{j,k}, \quad \delta_\alpha A_\beta f^n_{j,k} = A_\beta \delta_\alpha f^n_{j,k}, \quad \alpha, \beta \in \{x, y, t\}.$$

- Discrete Leibnitz rule in x-direction:

$$\delta_x (f^n_{j-1,k} \cdot g^n_{j,k}) = f^n_{j,k} \cdot \delta_x g^n_{j,k} + \delta_x f^n_{j-1,k} \cdot g^n_{j,k}, \tag{2.1}$$

$$\delta_x (f^n_{j,k} \cdot g^n_{j,k}) = f^n_{j,k} \cdot \delta_x g^n_{j,k} + \delta_x f^n_{j,k} \cdot g^n_{j+1,k}, \tag{2.2}$$

$$\delta_x (f^n_{j,k} \cdot g^n_{j,k}) = A_x f^n_{j,k} \cdot \delta_x g^n_{j,k} + \delta_x f^n_{j,k} \cdot A_x g^n_{j,k}. \tag{2.3}$$

Similarly, we can obtain a series of analogous discrete Leibnitz rules in space y-direction and time direction. These Leibnitz rules play an important role in proving the local structure property of the algorithm.

3. Local energy dissipation preserving algorithms

In this section, we apply the local structure-preserving algorithms proposed in [28,45] for the CH equation (1.1) to develop a series of local energy dissipation preserving algorithms.

3.1. Local energy dissipation preserving scheme I (LEDP-I)

To apply the local structure-preserving algorithm proposed in [28], we first introduce the intermediate variables $\mathbf{a} = \nabla\mu$ and $\mathbf{b} = \nabla\phi$, and rewrite the system (1.1) into the following first-order partial differential equation system

$$\begin{cases} \phi_t = \nabla\cdot\mathbf{a}, \quad \nabla\mu = \mathbf{a}, \\ \mu = f'(\phi) - \kappa\nabla\cdot\mathbf{b}, \quad \nabla\phi = \mathbf{b}, \end{cases} \tag{3.1}$$

which admits the following LEDL

$$\partial_t\left(\frac{\kappa}{2}|\nabla\phi|^2 + f(\phi)\right) - \nabla\cdot\left(\kappa\phi_t\mathbf{b} + \mu\mathbf{a}\right) + |\nabla\mu|^2 = 0. \tag{3.2}$$

Applying the implicit midpoint scheme in space and the discrete variational derivative method in time for the system (3.1) [11], we derive

$$\begin{cases} \delta_t A_x A_y \phi^n_{j,k} = \nabla_h\cdot(A_t\mathbf{a}^n_{j,k}), \\ \nabla_h(A_t\mu^n_{j,k}) = A_t A_x A_y \mathbf{a}^n_{j,k}, \\ A_t A_x A_y \mu^n_{j,k} = \frac{\delta f}{\delta(A_x A_y\phi^{n+1}_{j,k}, A_x A_y\phi^n_{j,k})} - \kappa\nabla_h\cdot(A_t\mathbf{b}^n_{j,k}), \\ \nabla_h(A_t\phi^n_{j,k}) = A_t A_x A_y \mathbf{b}^n_{j,k}, \end{cases} \tag{3.3}$$

where

$$\nabla_h = \begin{pmatrix} \delta_x A_y \\ \delta_y A_x \end{pmatrix}, \quad \frac{\delta f}{\delta(\phi,\psi)} = \begin{cases} \frac{f(\phi)-f(\psi)}{\phi-\psi}, & \text{if } \phi\neq\psi, \\ f'(\phi), & \text{if } \phi = \psi. \end{cases}$$

By eliminating the auxiliary variables, the scheme (3.3) can be recombined into a single equation

$$\delta_t A_x^4 A_y^4 \phi^n_{j,k} = \nabla_h^2\left(A_x A_y \frac{\delta f}{\delta(A_x A_y\phi^{n+1}_{j,k}, A_x A_y\phi^n_{j,k})} - \kappa\nabla_h^2(A_t\phi^n_{j,k})\right). \tag{3.4}$$

To evaluate the local energy dissipation law, we use the discretization of the form

$$\begin{aligned} LE^{n+1/2} = \max_{j,k}\Big|\delta_t\left(\frac{\kappa}{2}|\nabla_h\phi^n_{j,k}|^2 + f(A_x A_y\phi^n_{j,k})\right) \\ - \nabla'_h\cdot\left(\kappa\delta_t\phi^n_{j,k}A_t\mathbf{b}^n_{j,k} + A_t\mu^n_{j,k}A_t\mathbf{a}^n_{j,k}\right) + |\nabla_h(A_t\mu^n_{j,k})|^2\Big|, \end{aligned}$$

where

$$\nabla'_h\cdot(f^n_{j,k}\mathbf{a}^n_{j,k}) := \delta_x(A_y f^n_{j,k} A_y a1^n_{j,k}) + \delta_y(A_x f^n_{j,k} A_x a2^n_{j,k}),\ \mathbf{a} = (a_1, a_2)^T,$$

and

$$\nabla'_h\cdot(f^n_{j,k}\mathbf{a}^n_{j,k} + g^n_{j,k}\mathbf{b}^n_{j,k}) := \nabla'_h\cdot(f^n_{j,k}\mathbf{a}^n_{j,k}) + \nabla'_h\cdot(g^n_{j,k}\mathbf{b}^n_{j,k}).$$

$LE^{n+1/2}$ is called the maximal residual of LEDL. Next, we analyze properties of the above scheme.

Theorem 3.1. *The scheme (3.3) satisfies the following discrete LEDL*

$$\delta_t\left(\frac{\kappa}{2}|\nabla_h\phi^n_{j,k}|^2 + f(A_x A_y\phi^n_{j,k})\right) - \nabla'_h\cdot\left(\kappa\delta_t\phi^n_{j,k}A_t\mathbf{b}^n_{j,k} + A_t\mu^n_{j,k}A_t\mathbf{a}^n_{j,k}\right) + |\nabla_h(A_t\mu^n_{j,k})|^2 = 0. \tag{3.5}$$

Proof. Multiplying the four equations in (3.3) by $A_t A_x A_y\mu^n_{j,k}$, $\nabla_h(A_t\mu^n_{j,k})$, $-\delta_t A_x A_y\phi^n_{j,k}$ and $\kappa\nabla_h(\delta_t\phi^n_{j,k})$, respectively, we obtain

$$A_tA_xA_y\mu^n_{j,k}\cdot\delta_tA_xA_y\phi^n_{j,k}=A_xA_y(A_t\mu^n_{j,k})\cdot\nabla_h\cdot(A_t\mathbf{a}^n_{j,k}), \tag{3.6}$$

$$|\nabla_h(A_t\mu^n_{j,k})|^2=\nabla_h(A_t\mu^n_{j,k})\cdot A_xA_y(A_t\mathbf{a}^n_{j,k}), \tag{3.7}$$

$$-A_tA_xA_y\mu^n_{j,k}\cdot\delta_tA_xA_y\phi^n_{j,k}=-\delta_tf(A_xA_y\phi^n_{j,k})+\kappa A_xA_y(\delta_t\phi^n_{j,k})\cdot\nabla_h\cdot(A_t\mathbf{b}^n_{j,k}), \tag{3.8}$$

$$\kappa\nabla_h(A_t\phi^n_{j,k})\cdot\nabla_h(\delta_t\phi^n_{j,k})=\kappa\nabla_h(\delta_t\phi^n_{j,k})\cdot A_xA_y(A_t\mathbf{b}^n_{j,k}). \tag{3.9}$$

Adding the above four equations and thanks to the following Leibnitz rules

$$\delta_t(f^n\cdot g^n)=A_tf^n\cdot\delta_tg^n+\delta_tf^n\cdot A_tg^n,$$

$$\nabla'_h\cdot(f_{j,k}\mathbf{v}_{j,k})=A_xA_yf_{j,k}\cdot\nabla_h\cdot\mathbf{v}_{j,k}+\nabla_hf_{j,k}\cdot A_xA_y\mathbf{v}_{j,k},$$

we have complete the proof. □

Theorem 3.2. *Under the periodic boundary conditions, the scheme (3.3) conserves the discrete MCL*

$$\left(A_xA_y\phi^{n+1},1\right)_h=\left(A_xA_y\phi^n,1\right)_h, \tag{3.10}$$

and the discrete EDL

$$\delta_tE^n_h+\|\nabla_h(A_t\mu^n)\|^2_h=0, \tag{3.11}$$

where

$$E^n_h=\frac{\kappa}{2}\|\nabla_h\phi^n\|^2_h+\left(f(A_xA_y\phi^n),1\right)_h.$$

Proof. Summing the first equation of the scheme (3.3) and the discrete LEDL (3.5) over all indices j and k directly, respectively, and then combining the periodic boundary conditions, we obtain (3.10) and (3.11). This completes the proof. □

3.2. Concatenating method

In this subsection, we use the concatenating method [4,45] to construct local energy dissipation algorithms for the CH system (1.1). The main idea of the concatenating method is to rewrite the PDEs as a system of several simultaneous ODEs by introducing the auxiliary variables, then to concatenate different numerical methods for ODEs. We can rewrite the CH system (1.1) into the following ODEs:

$$\phi_t=a+b,\quad\begin{cases}c_x=a,\\ \mu_x=c,\end{cases}\quad\begin{cases}d_y=b,\\ \mu_y=d,\end{cases} \tag{3.12a}$$

$$\mu=f'(\phi)-\kappa(p+q),\quad\begin{cases}r_x=p,\\ \phi_x=r,\end{cases}\quad\begin{cases}s_y=q,\\ \phi_y=s,\end{cases} \tag{3.12b}$$

which admits the following LEDL

$$\partial_t\left(\frac{\kappa}{2}(\phi_x^2+\phi_y^2)+f(\phi)\right)-\partial_x\left(\kappa\phi_tr+\mu c\right)-\partial_y\left(\kappa\phi_ts+\mu d\right)+\mu_x^2+\mu_y^2=0. \tag{3.13}$$

3.2.1. Local energy dissipation preserving scheme II (LEDP-II)

In ODEs (3.12), applying the implicit point method, the discrete variational derivative method in time and the leap-frog scheme in space, we obtain

$$\delta_t\phi^n_{j,k}=A_ta^n_{j,k}+A_tb^n_{j,k}, \tag{3.14a}$$

$$\begin{cases}\delta_xc^n_{j,k}=a^n_{j,k},\\ \delta_x\mu^n_{j,k}=c^n_{j+1,k},\end{cases}\quad\begin{cases}\delta_yd^n_{j,k}=b^n_{j,k},\\ \delta_y\mu^n_{j,k}=d^n_{j,k+1},\end{cases} \tag{3.14b}$$

$$A_t\mu^n_{j,k}=\frac{\delta f}{\delta(\phi^{n+1}_{j,k},\phi^n_{j,k})}-\kappa(A_tp^n_{j,k}+A_tq^n_{j,k}), \tag{3.14c}$$

$$\begin{cases}\delta_xr^n_{j,k}=p^n_{j,k},\\ \delta_x\phi^n_{j,k}=r^n_{j+1,k},\end{cases}\quad\begin{cases}\delta_ys^n_{j,k}=q^n_{j,k},\\ \delta_y\phi^n_{j,k}=s^n_{j,k+1}.\end{cases} \tag{3.14d}$$

Eliminating the auxiliary variables, the scheme (3.14) can be recombined into a single equation

$$\delta_t \phi_{j,k}^n = \Delta_h \left(\frac{\delta f}{\delta(\phi_{j,k}^{n+1}, \phi_{j,k}^n)} - \kappa \Delta_h A_t \phi_{j,k}^n \right), \tag{3.15}$$

where

$$\Delta_h f_{j,k} := \delta_x^2 f_{j-1,k} + \delta_y^2 f_{j,k-1}.$$

Actually, when $f(\phi)$ is chosen as the double-well potential, the scheme proposed by Zhang and Qiao in [50] is a special case of (3.15). That is to say, the scheme in [50] can be derived by the concatenating method and conserves the discrete LEDL. Here we also define the maximal residual of LEDL for LEDP-II as follows

$$\begin{aligned} LE^{n+1/2} = \max_{j,k} \Big| & \delta_t \left(\frac{\kappa}{2} |\nabla_h^+ \phi_{j,k}^n|^2 + f(\phi_{j,k}^n) \right) \\ & - \nabla_h^+ \cdot \left(\kappa \delta_t \phi_{j,k}^n A_t \mathbf{b}_{j,k}^n + A_t \mu_{j,k}^n A_t \mathbf{a}_{j,k}^n \right) + |\nabla_h^+ (A_t \mu_{j,k}^n)|^2 \Big|, \end{aligned}$$

where

$$\nabla_h^+ := \begin{pmatrix} \delta_x \\ \delta_y \end{pmatrix}, \quad \mathbf{a} = \begin{pmatrix} c \\ d \end{pmatrix}, \quad \mathbf{b} = \begin{pmatrix} r \\ s \end{pmatrix}.$$

Next, we analyze properties of the scheme (3.14) or (3.15).

Theorem 3.3. *The scheme (3.14) possesses the following discrete LEDL*

$$\delta_t \left(\frac{\kappa}{2} |\nabla_h^+ \phi_{j,k}^n|^2 + f(\phi_{j,k}^n) \right) - \nabla_h^+ \cdot \left(\kappa \delta_t \phi_{j,k}^n A_t \mathbf{b}_{j,k}^n + A_t \mu_{j,k}^n A_t \mathbf{a}_{j,k}^n \right) + |\nabla_h^+ (A_t \mu_{j,k}^n)|^2 = 0. \tag{3.16}$$

Proof. By eliminating the variables a, b, p, q, the system (3.14) can be written as follows

$$\begin{cases} \delta_t \phi_{j,k}^n = A_t \delta_x c_{j,k}^n + A_t \delta_y d_{j,k}^n, \\ \delta_x \mu_{j,k}^n = c_{j+1,k}^n, \quad \delta_y \mu_{j,k}^n = d_{j,k+1}^n, \\ A_t \mu_{j,k}^n = \frac{\delta f}{\delta(\phi_{j,k}^{n+1}, \phi_{j,k}^n)} - \kappa (A_t \delta_x r_{j,k}^n + A_t \delta_y s_{j,k}^n), \\ \delta_x \phi_{j,k}^n = r_{j+1,k}^n, \quad \delta_y \phi_{j,k}^n = s_{j,k+1}^n. \end{cases} \tag{3.17}$$

Analogous to the proof of Theorem 3.1, we can deduce from (3.17) that

$$A_t \mu_{j,k}^n \cdot \delta_t \phi_{j,k}^n = A_t \mu_{j,k}^n \cdot \delta_x A_t c_{j,k}^n + A_t \mu_{j,k}^n \cdot \delta_y A_t d_{j,k}^n, \tag{3.18}$$

$$|\delta_x A_t \mu_{j,k}^n|^2 = \delta_x A_t \mu_{j,k}^n \cdot A_t c_{j+1,k}^n, \tag{3.19}$$

$$|\delta_y A_t \mu_{j,k}^n|^2 = \delta_y A_t \mu_{j,k}^n \cdot A_t d_{j,k+1}^n, \tag{3.20}$$

$$- A_t \mu_{j,k}^n \cdot \delta_t \phi_{j,k}^n = -\delta_t f(\phi_{j,k}^n) + \kappa (\delta_t \phi_{j,k}^n \cdot \delta_x A_t r_{j,k}^n + \delta_t \phi_{j,k}^n \cdot \delta_y A_t s_{j,k}^n), \tag{3.21}$$

$$\kappa \delta_x A_t \phi_{j,k}^n \cdot \delta_x \delta_t \phi_{j,k}^n = \kappa \delta_x \delta_t \phi_{j,k}^n \cdot A_t r_{j+1,k}^n, \tag{3.22}$$

$$\kappa \delta_y A_t \phi_{j,k}^n \cdot \delta_y \delta_t \phi_{j,k}^n = \kappa \delta_y \delta_t \phi_{j,k}^n \cdot A_t s_{j,k+1}^n. \tag{3.23}$$

Adding the above six equations, and then using the following Leibnitz rules we obtain

$$|\nabla_h^+ A_t \mu_{j,k}^n|^2 + \delta_t \left(\frac{\kappa}{2} |\nabla_h^+ \phi_{j,k}^n|^2 \right) = \nabla_h^+ \cdot (A_t \mu_{j,k}^n A_t \mathbf{a}_{j,k}^n) - \delta_t f(\phi_{j,k}^n) + \kappa \nabla_h^+ \cdot (\delta_t \phi_{j,k}^n A_t \mathbf{b}_{j,k}^n),$$

which leads to (3.16). □

Theorem 3.4. *Under the periodic boundary conditions, the scheme (3.14) conserves the following discrete MCL*

$$\left(\phi^{n+1}, 1\right)_h = \left(\phi^n, 1\right)_h, \tag{3.24}$$

and the discrete EDL

$$\delta_t E_h^n + \|\nabla_h^+ (A_t \mu^n)\|_h^2 = 0, \tag{3.25}$$

where

$$E_h^n = \frac{\kappa}{2} \|\nabla_h^+ \phi^n\|_h^2 + \left(f(\phi^n), 1\right)_h.$$

Proof. Summing the first equation of the system (3.17) and the discrete LEDL (3.16) over all indices j and k directly and then combining the periodic boundary conditions, we obtain (3.24) and (3.25). This completes the proof. □

3.2.2. Local energy dissipation preserving scheme III (LEDP-III)

Applying the implicit point method, the discrete variational derivative method in time and the leap-frog scheme and the implicit point method in space for (3.12a)–(3.12b), we obtain

$$\delta_t \phi^n_{j,k} = A_t a^n_{j,k} + A_t b^n_{j,k}, \tag{3.26a}$$

$$\begin{cases} \delta_x c^n_{j,k} = a^n_{j,k}, \\ \delta_x \mu^n_{j,k} = c^n_{j+1,k}, \end{cases} \quad \begin{cases} \delta_y d^n_{j,k} = b^n_{j,k}, \\ \delta_y \mu^n_{j,k} = d^n_{j,k+1}, \end{cases} \tag{3.26b}$$

$$A_t A_x A_y \mu^n_{j,k} = \frac{\delta f}{\delta (A_x A_y \phi^{n+1}_{j,k}, A_x A_y \phi^n_{j,k})} - \kappa (A_t A_x A_y p^n_{j,k} + A_t A_x A_y q^n_{j,k}), \tag{3.26c}$$

$$\begin{cases} \delta_x r^n_{j,k} = A_x p^n_{j,k}, \\ \delta_x \phi^n_{j,k} = A_x r^n_{j,k}, \end{cases} \quad \begin{cases} \delta_y s^n_{j,k} = A_y q^n_{j,k}, \\ \delta_y \phi^n_{j,k} = A_y s^n_{j,k}. \end{cases} \tag{3.26d}$$

Eliminating the auxiliary variables, we obtain an equivalent scheme

$$\delta_t A_x^2 A_y^2 \phi^n_{j,k} = \Delta_h \left(A_x A_y \frac{\delta f}{\delta (A_x A_y \phi^{n+1}_{j,k}, A_x A_y \phi^n_{j,k})} - \kappa \nabla_h^2 (A_t \phi^n_{j,k}) \right). \tag{3.27}$$

Similarly, we can define the maximal residual of LEDL for LEDP-III as the following

$$\begin{aligned} LE^{n+1/2} = \max_{j,k} \Big| & \delta_t \left(\frac{\kappa}{2} |\nabla_h \phi^n_{j,k}|^2 + f(A_x A_y \phi^n_{j,k}) \right) - \kappa \nabla_h' \cdot (\delta_t \phi^n_{j,k} A_t \mathbf{b}^n_{j,k}) \\ & - \nabla_h^+ \cdot \left(A_t A_x A_y \mu^n_{j,k} A_t A_x A_y \mathbf{a}^n_{j,k} \right) + |\nabla_h^+ (A_t A_x A_y \mu^n_{j,k})|^2 \Big|, \end{aligned}$$

where

$$\mathbf{a} = \begin{pmatrix} c \\ d \end{pmatrix}, \quad \mathbf{b} = \begin{pmatrix} r \\ s \end{pmatrix}.$$

Next, we analyze properties of the scheme (3.26).

Theorem 3.5. *The scheme (3.26) possesses the following discrete LEDL*

$$\begin{aligned} & \delta_t \left(\frac{\kappa}{2} |\nabla_h \phi^n_{j,k}|^2 + f(A_x A_y \phi^n_{j,k}) \right) - \kappa \nabla_h' \cdot (\delta_t \phi^n_{j,k} A_t \mathbf{b}^n_{j,k}) \\ & - \nabla_h^+ \cdot \left(A_t A_x A_y \mu^n_{j,k} A_t A_x A_y \mathbf{a}^n_{j,k} \right) + |\nabla_h^+ (A_t A_x A_y \mu^n_{j,k})|^2 = 0. \end{aligned} \tag{3.28}$$

Proof. By eliminating the variables a, b, p, q, the system (3.26) can be written as follows

$$\begin{cases} \delta_t \phi^n_{j,k} = A_t \delta_x c^n_{j,k} + A_t \delta_y d^n_{j,k}, \\ \delta_x \mu^n_{j,k} = c^n_{j+1,k}, \quad \delta_y \mu^n_{j,k} = d^n_{j,k+1}, \\ A_t A_x A_y \mu^n_{j,k} = \frac{\delta f}{\delta (A_x A_y \phi^{n+1}_{j,k}, A_x A_y \phi^n_{j,k})} - \kappa \nabla_h \cdot (A_t \mathbf{b}^n_{j,k}), \\ \nabla_h (A_t \phi^n_{j,k}) = A_t A_x A_y \mathbf{b}^n_{j,k}. \end{cases} \tag{3.29}$$

Analogous to the proof of Theorem 3.1, we can deduce from (3.29)

$$\begin{aligned} & A_t A_x A_y \mu^n_{j,k} \cdot \delta_t A_x A_y \phi^n_{j,k} = A_t A_x A_y \mu^n_{j,k} \cdot \delta_x A_t A_x A_y c^n_{j,k} + A_t A_x A_y \mu^n_{j,k} \cdot \delta_y A_t A_x A_y d^n_{j,k}, \\ & |\delta_x A_t A_x A_y \mu^n_{j,k}|^2 = \delta_x A_t A_x A_y \mu^n_{j,k} \cdot A_t A_x A_y c^n_{j+1,k}, \\ & |\delta_y A_t A_x A_y \mu^n_{j,k}|^2 = \delta_y A_t A_x A_y \mu^n_{j,k} \cdot A_t A_x A_y d^n_{j,k+1}, \\ & - A_t A_x A_y \mu^n_{j,k} \cdot \delta_t A_x A_y \phi^n_{j,k} = -\delta_t f(A_x A_y \phi^n_{j,k}) + \kappa A_x A_y (\delta_t \phi^n_{j,k}) \cdot \nabla_h \cdot (A_t \mathbf{b}^n_{j,k}), \\ & \kappa \nabla_h (A_t \phi^n_{j,k}) \cdot \nabla_h (\delta_t \phi^n_{j,k}) = \kappa \nabla_h (\delta_t \phi^n_{j,k}) \cdot A_x A_y (A_t \mathbf{b}^n_{j,k}). \end{aligned}$$

Adding the above five equations, and then using some discrete Leibnitz rules, we obtain (3.28). This completes the proof. □

Theorem 3.6. *Under the periodic boundary conditions, the scheme (3.26) conserves the following discrete MCL*

$$\left(\phi^{n+1}, 1\right)_h = \left(\phi^n, 1\right)_h, \tag{3.30}$$

Table 1
Mesh refinement test of the scheme I at $T = 1$ with fixed $\Delta t = 0.001$.

N	L^∞-error	L^2-error	L^∞-order	L^2-order	CPU (s)
11	6.4688e−02	1.6836e−01	–	–	1.38
33	6.1165e−03	1.7115e−02	2.1469	2.0810	2.66
99	6.7016e−04	1.8833e−03	2.0127	2.0088	13.28
297	7.4395e−05	2.0919e−04	2.0008	2.0003	46.12

Table 2
Mesh refinement test of the scheme I at $T = 1$ with fixed $N = 2001$.

Δt	L^∞-error	L^2-error	L^∞-order	L^2-order	CPU (s)
0.2	2.4072e−03	7.2618e−03	–	–	33.14
0.1	5.3057e−04	1.8073e−03	2.1817	2.0065	41.56
0.05	1.3535e−04	4.5441e−04	1.9709	1.9918	88.89
0.025	3.5066e−05	1.1698e−04	1.9485	1.9577	148.52

Table 3
Mesh refinement test of the scheme II at $T = 1$ with fixed $\Delta t = 0.001$.

N	L^∞-error	L^2-error	L^∞-order	L^2-order	CPU (s)
11	3.3894e−02	1.0464e−01	–	–	1.12
33	3.7356e−03	1.1623e−02	2.0074	2.0003	2.29
99	4.1475e−04	1.2913e−03	2.0007	2.0001	11.77
297	4.6127e−05	1.4363e−04	1.9991	1.9990	28.12

and the discrete EDL

$$\delta_t E_h^n + \|\nabla_h^+ (A_t A_x A_y \mu^n)\|_h^2 = 0, \tag{3.31}$$

where

$$E_h^n = \frac{\kappa}{2}\|\nabla_h \phi^n\|_h^2 + \left(f(A_x A_y \phi^n), 1\right)_h.$$

Proof. Summing the first equation of the system (3.29) and the discrete LEDL (3.28) over all indices j and k directly, and then combining the periodic boundary conditions, we obtain (3.30) and (3.31). This completes the proof. □

Remark 3.1. In this work, we construct the three local structure-preserving algorithms, which are the natural generalization of the corresponding global structure-preserving algorithms. Under the suitable boundary conditions, local structure-preserving algorithms for the PDEs are global structure-preserving algorithms, but the inverse is not necessarily valid.

4. Numerical experiments

In this section, we present some numerical results to illustrate the efficiency and accuracy of the proposed methods. We notice that the proposed methods lead to nonlinear algebraic systems, which can be solved using simple fixed-point iterative methods (see [29]). Due to periodic boundary conditions, the fast Fourier transform can be applied for every iteration step. In the following experiments, we take $f(\phi) = \frac{\gamma}{4}(1-\phi^2)^2$.

Example 4.1. In order to test the convergence rate, we first consider the system (1.1) with the double well free energy in a rectangular domain $[0, 2\pi] \times [0, 2\pi]$ till time $T = 1$ and make the following exact solution of the system modified by a appropriate forcing function

$$\phi(x, y, t) = \cos(x)\cos(y)\cos(t). \tag{4.1}$$

The parameter values are chosen as $\gamma = \kappa = 1$. Here, we choose the number of the spatial grids as $N_x = N_y = N$. In Tables 1–6, we compare the numerical solution with the exact solution at $T = 1$, and compute the discrete L^2 and L^∞ errors of phase variable ϕ by varying the grid size in space and time, respectively. From Tables 1–6, we observe that all proposed schemes are second-order accurate in both time and space. In this example, the scheme II is slightly more accurate than the scheme III, while the scheme III is better than the scheme I.

Example 4.2. In this example, we consider the system (1.1) with the double well free energy to study coalescence of two drops. The problem is solved in the space domain $[0, 1] \times [0, 1]$ with the initial condition

Table 4
Mesh refinement test of the scheme II at $T = 1$ with fixed $N = 2001$.

Δt	L^∞-error	L^2-error	L^∞-order	L^2-order	CPU (s)
0.2	2.4060e−03	7.2603e−03	–	–	20.73
0.1	5.3002e−04	1.8058e−03	2.1826	2.0074	28.89
0.05	1.3472e−04	4.5299e−04	1.9760	1.9951	46.99
0.025	3.4444e−05	1.1557e−04	1.9677	1.9707	85.57

Table 5
Mesh refinement test of the scheme III at $T = 1$ with fixed $\Delta t = 0.001$.

N	L^∞-error	L^2-error	L^∞-order	L^2-order	CPU (s)
11	4.8796e−02	1.3097e−01	–	–	1.22
33	4.8948e−03	1.3659e−02	2.0931	2.0577	2.54
99	5.3856e−04	1.5077e−03	2.0089	2.0060	13.15
297	5.9823e−05	1.6756e−04	2.0003	1.9998	39.62

Table 6
Mesh refinement test of the scheme III at $T = 1$ with fixed $N = 2001$.

Δt	L^∞-error	L^2-error	L^∞-order	L^2-order	CPU (s)
0.2	2.4067e−03	7.2608e−03	–	–	24.00
0.1	5.3007e−04	1.8063e−03	2.1822	2.0071	34.36
0.05	1.3503e−04	4.5349e−04	1.9735	1.9939	56.90
0.025	3.4745e−05	1.1607e−04	1.9583	1.9661	112.86

$$\phi(x, y, 0) = \begin{cases} \tanh\big((0.2 - r_1)/\delta\big), & r_1 < 0.2 + \delta, \\ \tanh\big((0.2 - r_2)/\delta\big), & r_2 < 0.2 + \delta, \\ -1, & \text{other}, \end{cases}$$

where $r_1 = \sqrt{(x - 0.3 + \delta)^2 + (y - 0.5)^2}$, $r_2 = \sqrt{(x - 0.7 - \delta)^2 + (y - 0.5)^2}$ and $\delta = 0.01$. The parameters are taken as $\gamma = 0.1$, $\kappa = 1.0e{-}5$.

To compare the proposed schemes, we compute the discrete mass error and energy by using the following unified formula, respectively,

$$R_M^n = \big|(\phi^n, 1)_h - (\phi^0, 1)_h\big|,$$
$$E_h^n = \frac{\kappa}{2}\|\nabla_h^+ \phi^n\|_h^2 + \big(f(\phi^n), 1\big)_h.$$

To investigate the discrete local energy dissipation law, we calculate the maximal residual of LEDL of the three methods defined in the previous section. Figs. 1–3 present the evolution of drops obtained using the three proposed methods with $N_x = N_y = 129$, $\Delta t = 0.0001$, respectively. We show the numerical solution at $t = 0, 1, 3, 5, 10, 30$. These figures show that the evolutions of drops by the three methods are essentially identical. The two equal-sized circular drops coalesce quickly in the early stage of the evolution, and slowly later until they eventually merge into a single one. The errors in the total mass, the energy change and the maximal residual of LEDL with respect to time are plotted. As can be seen from Fig. 4 (a)–(b), the mass is numerically conservative in three cases, while energy decays with the same trajectory. Fig. 4 (c) shows that the LEDP-II and the LEDP-III have outstanding performance in conserving the local energy dissipation law. Through numerical experiments, we observe that the LEDP-II and the LEDP-III perform very well.

Remark 4.1. In the numerical implementations, the fixed-point iterative technique proposed in [29] is applied for solving our nonlinear schemes, where the iterative termination criteria is taken as $\|\phi^{n+1,s+1} - \phi^{n+1,s}\|_\infty < TOL$. In this example, we set $TOL = 1.0e{-}11$ for the scheme I, and $TOL = 1.0e{-}14$ for the scheme II and the scheme III. We find that the nonlinear iteration for the scheme I doesn't work if we take $TOL < 1.0e{-}11$. As can be seen from Fig. 4 (c), the maximum residual of the scheme I is close to $1.0e{-}4$, which may be due to the accumulation of numerical iteration error.

Example 4.3. Here we consider coarsening dynamics. The initial condition is a random state by assigning a random number varying from -0.1 to 0.1 to each grid point. We take the parameters $\gamma = 0.1, \kappa = 1.0e{-}5$, and the domain $[0, 1] \times [0, 1]$.

The space grid is taken as 129×129 and the time step is $\Delta t = 0.0001$. In Fig. 5, we only show the numerical solution obtained using the scheme (3.27) in some selected time moments. The two phases are not well-separated initially in the given initial condition. Over time, they quickly separate and coarsen into one phase in droplets immersed in the other phase. In the end, it reaches a steady state. It can also be reflected from the energy evolution which is presented in Fig. 6.

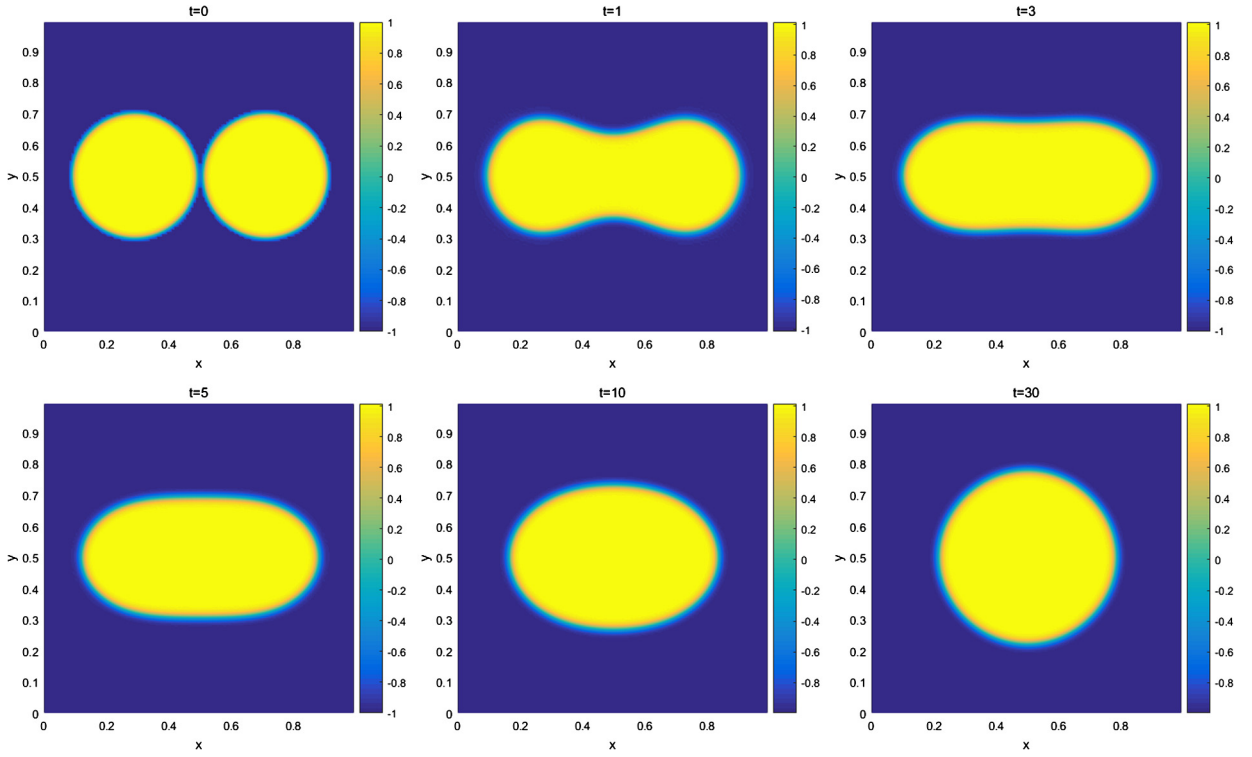

Fig. 1. Coalescence of two drops simulated using LEDP-I with $N = 129$, $\Delta t = 0.0001$.

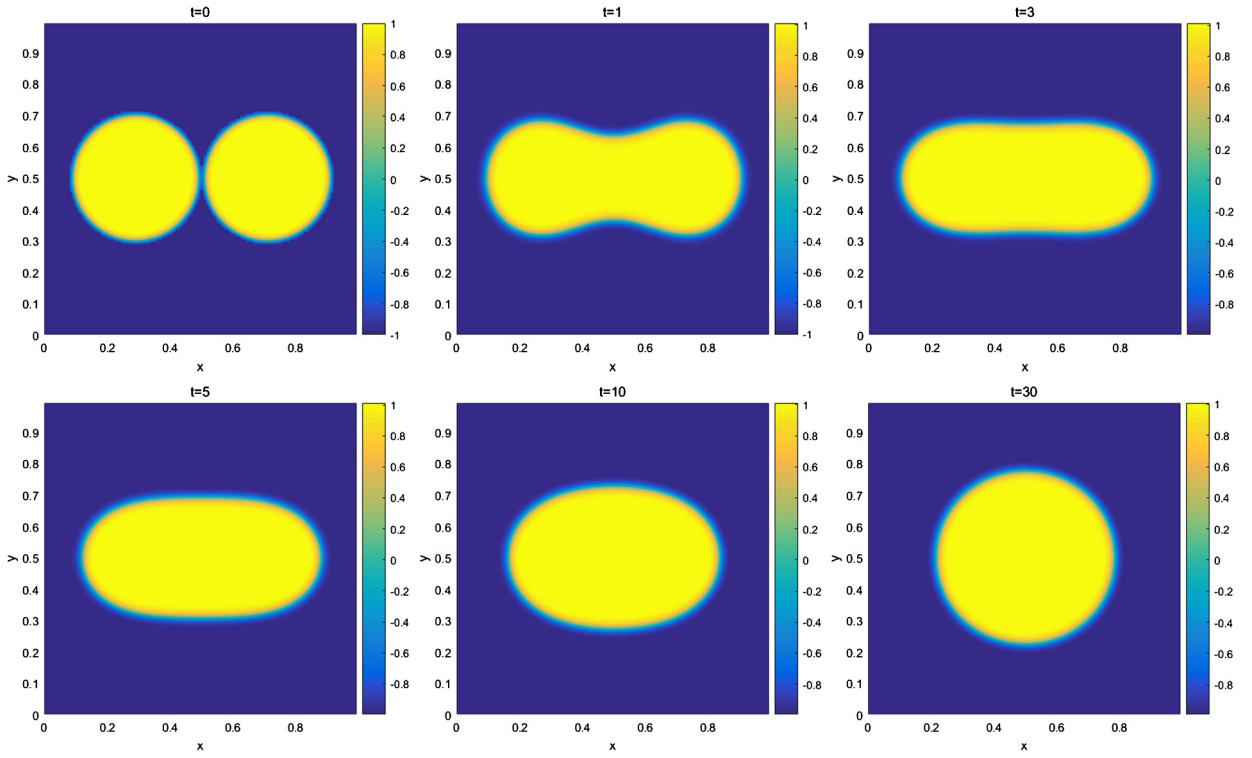

Fig. 2. Coalescence of two drops simulated using LEDP-II with $N = 129$, $\Delta t = 0.0001$.

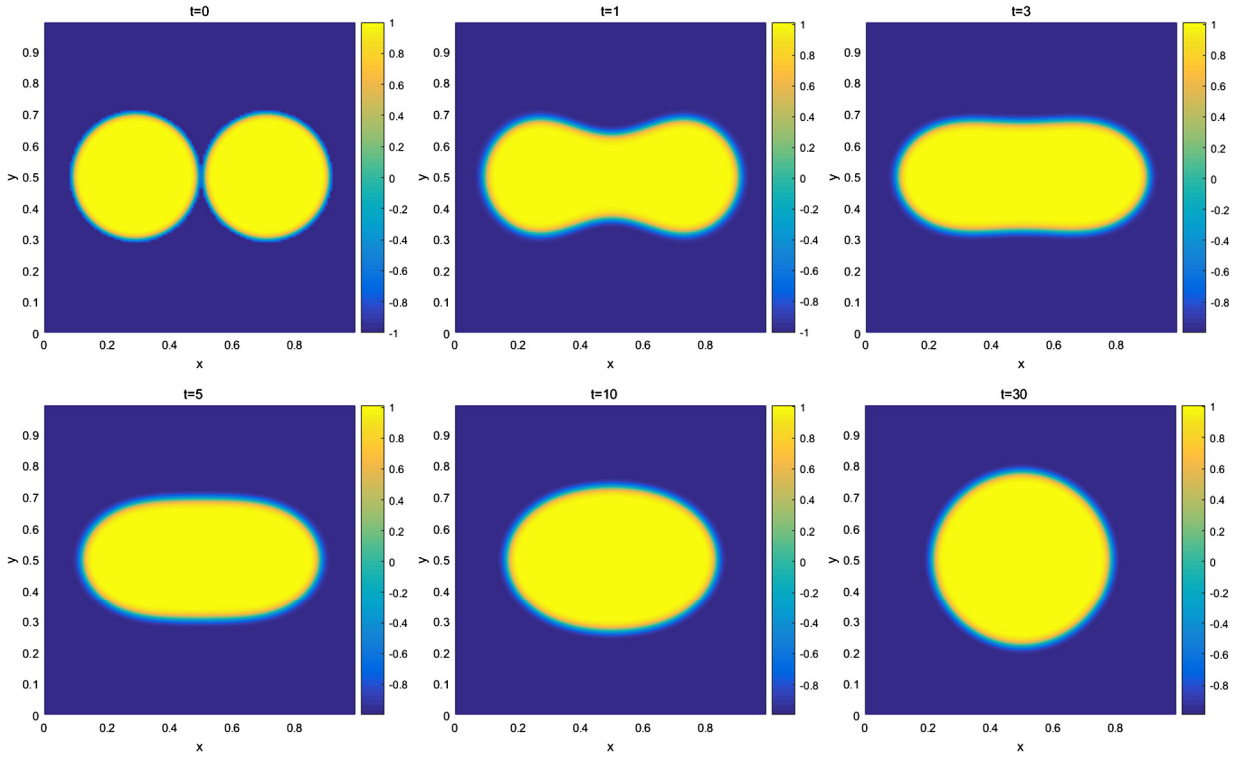

Fig. 3. Coalescence of two drops simulated using LEDP-III with $N = 129$, $\Delta t = 0.0001$.

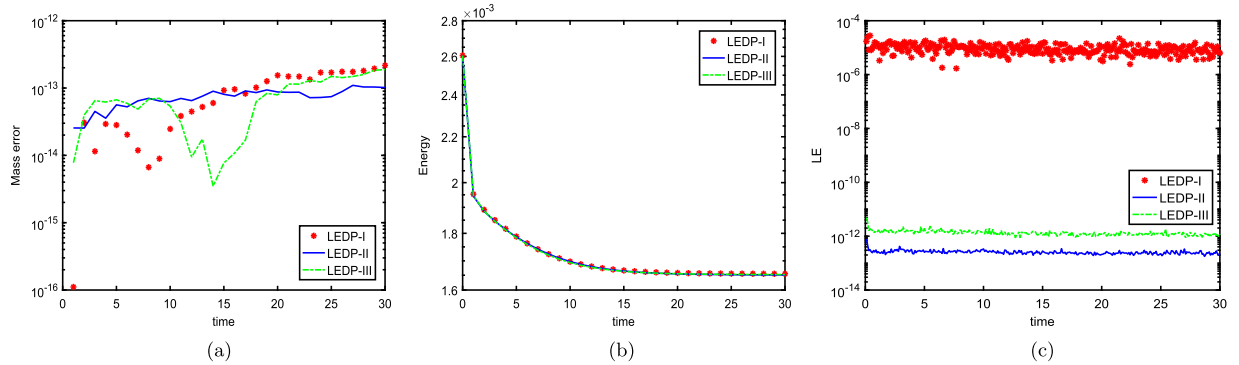

Fig. 4. Comparison between the three schemes with $N = 129$, $\Delta t = 0.0001$ in the drop coalescence example. (a) Mass error. (b) The evolution of energy. (c) The maximal residual of local energy dissipation law.

5. Concluding remarks

In this paper, we observe that the CH equation possesses a local energy dissipation law. Based on this observation, we derive the three LEDL numerical schemes for the 2D CH equation by the concatenating method. In particular, when the nonlinear bulk potential function $f(\phi)$ is chosen as the double-well potential, the method [50] proposed by Zhang and Qiao is a special case of our scheme II, which means the method [50] possesses a local property. Utilizing the discrete Leibnitz rule and the properties of operators, we rigorously prove the constructed schemes admit the discrete LEDL in any time–space region. As the equation subjects to periodic boundary conditions, the newly derived schemes are shown to conserve the discrete total mass conservation and energy dissipation law. Numerical results indicate that our schemes not only provide accurate solutions in long-term computations, but also have excellent preservations of local energy dissipation rate. Later, we will try to give error estimates of these newly derived local structure-preserving algorithms.

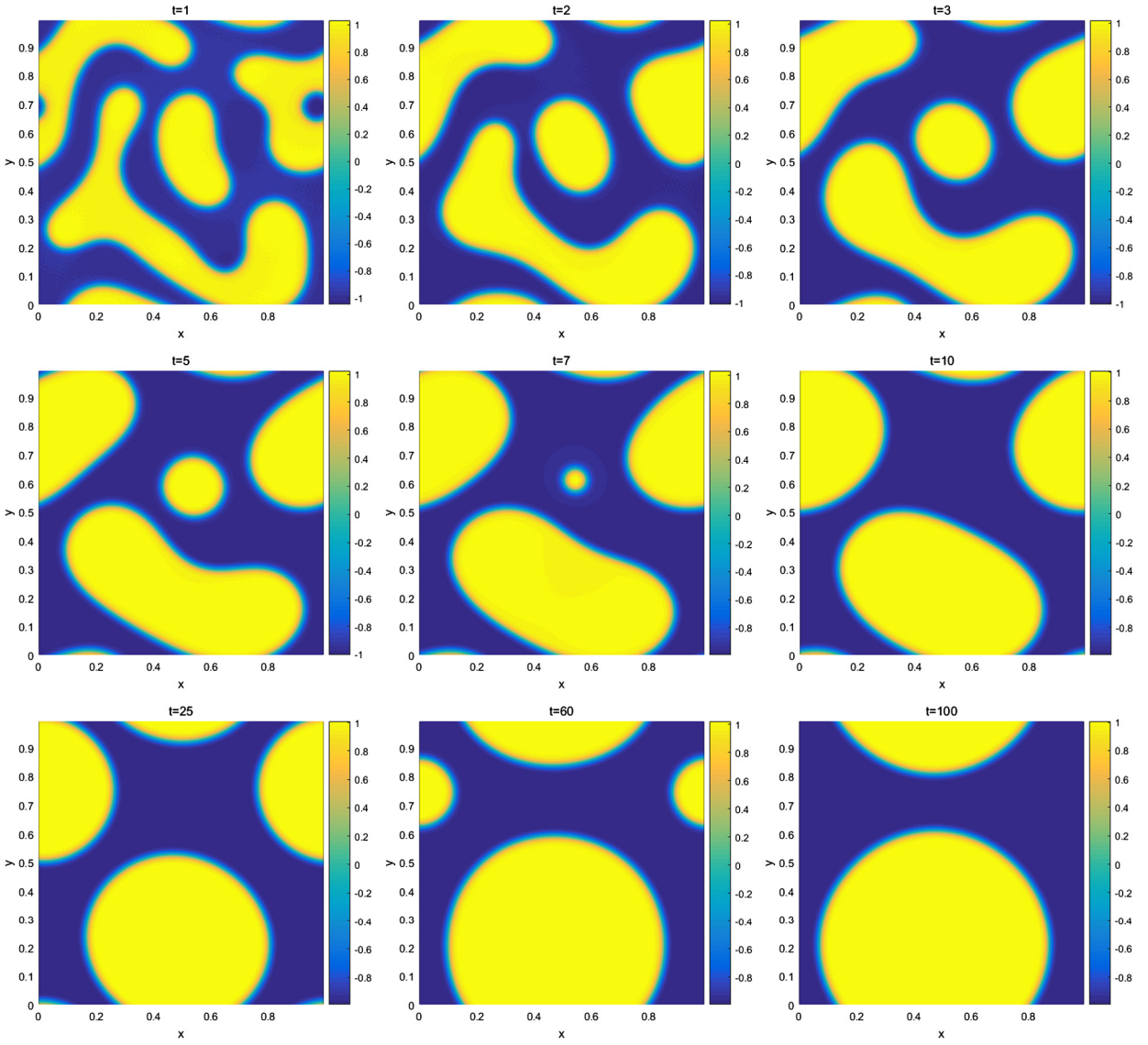

Fig. 5. Coarsening dynamics simulated using LEDP-III with $N = 129$, $\Delta t = 0.0001$.

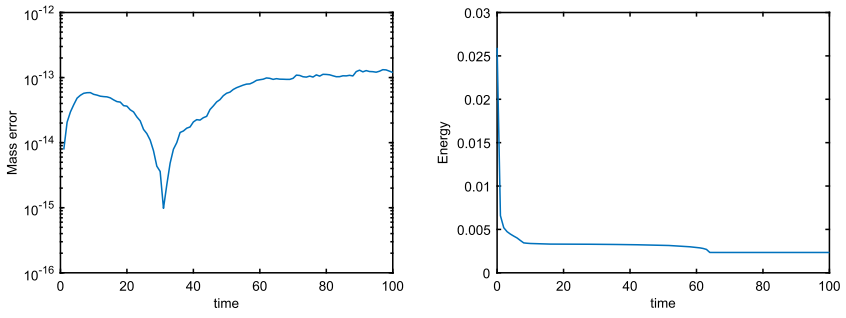

Fig. 6. The mass error and evolution of energy in the coarsening dynamics.

Acknowledgements

This work is supported by the National Natural Science Foundation of China (under Grant Nos. 11771213 and 41504078), the National Key Research and Development Project of China (under Grant No. 2016YFC0600310), the Natural Science Foundation of Jiangsu Province (Grant No. SBK2018040413), the Major Projects of Natural Sciences of University in Jiangsu Province of China (Grant No. 15KJA110002) and the Priority Academic Program Development of Jiangsu Higher Education Institutions, China.

References

[1] D.M. Anderson, G.B. McFadden, A.A. Wheeler, Diffuse-interface methods in fluid mechanics, Annu. Rev. Fluid Mech. 30 (1998) 139–165.
[2] J. Bosch, C. Kahle, M. Stoll, Preconditioning of a coupled Cahn–Hilliard Navier–Stokes system, Commun. Comput. Phys. 23 (2018) 603–628.
[3] J.W. Cahn, Free energy of a nonuniform system. II. Thermodynamic basis, J. Chem. Phys. 30 (1959) 1121–1124.
[4] J.X. Cai, Y.S. Wang, H. Liang, Local energy-preserving and momentum-preserving algorithms for coupled nonlinear Schrödinger system, J. Comput. Phys. 239 (2013) 30–50.
[5] S.M. Choo, S.K. Chung, K.I. Kim, Conservative nonlinear difference scheme for the Cahn–Hilliard equation-II, Comput. Math. Appl. 39 (2000) 229–243.
[6] J.W. Cahn, J.E. Hilliard, Free energy of a nonuniform system. I. Interfacial energy free energy, J. Chem. Phys. 31 (1959) 688–699.
[7] A. Christlieb, J. Jones, K. Promislow, B. Wetton, M. Willoughby, High accuracy solutions to energy gradient flows from material science models, J. Comput. Phys. 257 (2014) 193–215.
[8] L.Q. Chen, J. Shen, Applications of semi-implicit Fourier-spectral method to phase field equations, Comput. Phys. Commun. 108 (1998) 147–158.
[9] F. Chen, J. Shen, Efficient energy stable schemes with spectral discretization in space for anisotropic Cahn–Hilliard systems, Commun. Comput. Phys. 13 (2013) 1189–1208.
[10] K.L. Cheng, C. Wang, S.M. Wise, X.Y. Yue, A second-order, weakly energy-stable pseudo-spectral scheme for the Cahn–Hilliard equation and its solution by the homogeneous linear iteration method, J. Sci. Comput. 69 (2016) 1083–1114.
[11] M. Dahlby, B. Owren, A general framework for deriving integral preserving numerical methods for PDEs, SIAM J. Sci. Comput. 33 (2011) 2318–2340.
[12] C.M. Elliott, D.A. French, Numerical studies of the Cahn–Hilliard equation for phase separation, IMA J. Appl. Math. 38 (1987) 97–128.
[13] C.M. Elliott, Z. Sonqmu, On the Cahn–Hilliard equation, Arch. Ration. Mech. Anal. 96 (1986) 339–357.
[14] C.M. Elliott, A.M. Stuart, The global dynamics of discrete semilinear parabolic equations, SIAM J. Numer. Anal. 30 (1993) 1622–1663.
[15] D. Eyre, Unconditionally gradient stable time marching the Cahn–Hilliard equation, Comput. Math. Models Microstruct. Evol. 529 (1998) 39–46.
[16] D. Furihata, A stable and conservative finite difference scheme for the Cahn–Hilliard equation, Numer. Math. 87 (2001) 675–699.
[17] X.B. Feng, A. Prohl, Error analysis of a mixed finite element method for the Cahn–Hilliard equation, Numer. Math. 99 (2004) 47–84.
[18] D. Furihata, Finite difference schemes for $\frac{\partial u}{\partial t} = (\frac{\partial}{\partial x})^{\alpha} \frac{\delta G}{\delta u}$ that inherit energy conservation or dissipation property, J. Comput. Phys. 156 (1999) 181–205.
[19] W.M. Feng, P. Yu, S.Y. Hu, Z.K. Liu, Q. Du, L.Q. Chen, A Fourier spectral moving mesh method for the Cahn–Hilliard equation with elasticity, Commun. Comput. Phys. 5 (2009) 582–599.
[20] M.G. Forest, Q. Wang, X.F. Yang, Lcp droplet dispersions: a two-phase, diffuse-interface kinetic theory and global droplet defect predictions, Soft Matter 8 (2012) 9642–9660.
[21] H. Gomez, T.J.R. Hughes, Provably unconditionally stable, second-order time-accurate, mixed variational methods for phase-field models, J. Comput. Phys. 230 (2011) 5310–5327.
[22] M.E. Gurtin, D. Polignone, J. Vinals, Two-phase binary fluids and immiscible fluids described by an order parameter, Math. Models Methods Appl. Sci. 6 (1996) 815–831.
[23] H. Gomez, K. van der Zee, Computational phase-field modeling, in: Encyclopedia of Computational Mechanics, 2nd edition, 2017.
[24] J. Carr, M.E. Gurtin, M. Slemrod, Structured phase transitions on a finite interval, Arch. Ration. Mech. Anal. 86 (1984) 317–351.
[25] F. Guilln-Gonzlez, G. Tierra, On linear schemes for a Cahn–Hilliard diffuse interface model, J. Comput. Phys. 234 (2013) 140–171.
[26] F. Guilln-Gonzlez, G. Tierra, Second order schemes and time-step adaptivity for Allen–Cahn and Cahn–Hilliard models, Comput. Math. Appl. 68 (2014) 821–846.
[27] J. Guo, C. Wang, S.M. Wise, X. Yue, An H^2 convergence of a second-order convexsplitting, finite difference scheme for the three-dimensional Cahn–Hilliard equation, Commun. Math. Sci. 14 (2015) 489–515.
[28] Y.Z. Gong, J.X. Cai, Y.S. Wang, Some new structure-preserving algorithms for general multi-symplectic formulations of Hamiltonian PDEs, J. Comput. Phys. 279 (2014) 80–102.
[29] Y. Gong, Q. Wang, Y. Wang, J. Cai, A conservative Fourier pseudo-spectral method for the nonlinear Schrödinger equation, J. Comput. Phys. 328 (2017) 354–370.
[30] D.Z. Han, A. Brylev, X.F. Yang, Z.J. Tan, Numerical analysis of second order, fully discrete energy stable schemes for phase field models of two phase incompressible flows, J. Sci. Comput. 70 (2017) 965–989.
[31] Y.N. He, Y.X. Liu, T. Tang, On large time-stepping methods for the Cahn–Hilliard equation, Appl. Numer. Math. 57 (2007) 616–628.
[32] L.L. Ju, J. Zhang, Q. Du, Fast and accurate algorithms for simulating coarsening dynamics of Cahn–Hilliard equations, Comput. Mater. Sci. 108 (2015) 272–282.
[33] J. Kim, Phase-field models for multi-component fluid flows, Commun. Comput. Phys. 12 (2012) 613–661.
[34] J. Liu, C.M. Landis, H. Gomez, Thomas J.R. Hughes, Liquid-vapor phase transition: thermomechanical theory, entropy stable numerical formulation, and boiling simulations, Comput. Methods Appl. Mech. Eng. 297 (2015) 476–553.
[35] D. Li, Z.H. Qiao, On second order semi-implicit Fourier spectral methods for 2d Cahn–Hilliard equations, J. Sci. Comput. 70 (2017) 1–41.
[36] D. Li, Z.H. Qiao, T. Tang, Characterizing the stabilization size for semi-implicit Fourier-spectral method to phase field equations, SIAM J. Numer. Anal. 54 (2016) 1653–1681.
[37] C. Liu, J. Shen, A phase field model for the mixture of two incompressible fluids and its approximation by a Fourier-spectral method, Physica D 179 (2003) 211–228.
[38] L. Ma, R. Chen, X.F. Yang, H. Zhang, Numerical approximations for Allen–Cahn type phase field model of two-phase incompressible fluids with moving contact lines, Commun. Comput. Phys. 21 (2017) 867–889.
[39] L. Rayleigh, On the theory of surface forces-II. Compressible fluids, Philos. Mag. 33 (1976) 209–220.
[40] Z.Z. Sun, A second-order accurate linearized difference scheme for the two-dimensional Cahn–Hilliard equation, Math. Comput. 64 (1995) 1463–1471.
[41] R. Scala, G. Schimperna, On the viscous Cahn–Hilliard equation with singular potential and inertial term, AIMS Math. 1 (1) (2016) 64–76, https://doi.org/10.3934/Math.2016.1.64.
[42] J. Shen, X.F. Yang, Numerical approximations of Allen–Cahn and Cahn–Hilliard equations, Discrete Contin. Dyn. Syst. 28 (2012) 1669–1691.
[43] P.C. Song, T.N. Yang, Y.Z. Ji, Z. Wang, Z.G. Yang, L.Q. Chen, L. Chen, A comparison of Fourier spectral iterative perturbation method and finite element method in solving phase-field equilibrium equations, Commun. Comput. Phys. 21 (2017) 1325–1349.

[44] J. van der Waals, The thermodynamic theory of capillarity under the hypothesis of a continuous density variation, J. Stat. Phys. 20 (1893) 197–244.
[45] Y.S. Wang, B. Wang, M.Z. Qin, Local structure-preserving algorithms for partial differential equations, Sci. China Ser. A 51 (2008) 2115–2136.
[46] X.F. Yang, Linear, first and second-order, unconditionally energy stable numerical schemes for the phase field model of homopolymer blends, J. Comput. Phys. 327 (2016) 294–316.
[47] P.T. Yue, J.J. Feng, C. Liu, J. Shen, A diffuse-interface method for simulating two-phase flows of complex fluids, J. Fluid Mech. 515 (2004) 293–317.
[48] J. Zhao, X.F. Yang, Y.Z. Gong, Q. Wang, A novel linear second order unconditionally energy stable scheme for a hydrodynamic Q-tensor model of liquid crystals, Comput. Methods Appl. Mech. Eng. 318 (2017) 803–825.
[49] J.Z. Zhu, L.Q. Chen, J. Shen, V. Tikare, Coarsening kinetics from a variable-mobility Cahn–Hilliard equation: application of a semi-implicit Fourier spectral method, Phys. Rev. (1999) 3564–3572.
[50] Z.R. Zhang, Z.H. Qiao, An adaptive time-stepping strategy for the Cahn–Hilliard equation, Commun. Comput. Phys. 11 (2012) 1261–1278.